Title
Photocatalytic dechlorination of unactivated chlorocarbons including PVC using organolanthanide complexes

Journal
Chemical Communications, 59(73)

ISSN
1359-7345

Authors
Kynman, Amy E
Christodoulou, Stella
Ouellette, Erik T
et al.

Publication Date
2023-09-12

DOI
10.1039/d3cc02906a

Photocatalytic dechlorination of unactivated chlorocarbons including PVC using organolanthanide complexes

Amy E. Kynman,[a,b] Stella Christodoulou,[c] Erik T. Ouellette,[a,b] Appie Peterson,[b] Sheridon N. Kelly, [a,b] Laurent Maron[c] and Polly Arnold [a,b*]

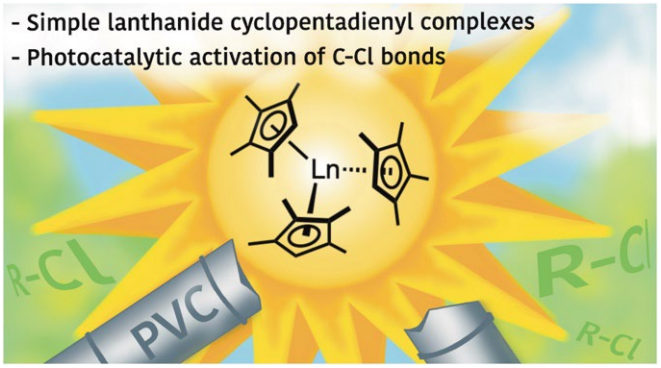

Simple lanthanide cyclopentadienyl (Cp) complexes can photochemically cleave the sp³ carbon-chlorine bond of unactivated chlorinated hydrocarbons including polyvinyl chloride (PVC). The excited state lifetimes of these simple complexes are among the longest observed for cerium complexes (175 ns for $[(Cp^{Me4})_2Ce(\mu\text{–}Cl)]_2$) and the light absorption by the Cp ligand is efficient, so photocatalytic reactivity is enhanced for cerium and now also made possible for neighboring, normally photoinactive, lanthanide congeners.

Photoredox catalysis provides versatile and energy-efficient routes for the synthesis of complex molecules.[1–3] Modern photocatalysts can undergo single electron transfer (SET) processes following irradiation with UV, or more desirably visible light, enabling challenging chemical transformations to be accessed under milder conditions than thermally driven reactions.[4]

The use of lanthanides in catalysis is desirable due to the relative abundance of many and their low toxicity.[5–8] Their halophilicity has led us and others to explore their potential for catalytic carbon–halogen functionalization reactions. Early work showed that under light irradiation at 40 °C, SmI_2 can reductively dechlorinate 1-chlorodocecane.[9] Divalent $Ln(Cp^*)_2$ (Ln = Sm, Eu, and Yb, $Cp^* = C_5Me_5$), were shown to cleave C–Cl bonds forming the Ln(III) halide, and the reaction could be made catalytic under high energy (near UV) irradiation.[10–12]

The strong Ln–Cl bond can provide an additional driving force to reactions that cleave the strong sp³C–Cl bond which would be unreactive according to the redox potentials. Photoredox catalysis by lanthanide complexes, using low energy, visible light is underexploited, and simple Ce(III) coordination complexes dominate the studies.[13–15] Cerium possesses both an accessible (III)/(IV) redox couple and an allowed $4f^1$ ground to $5d^1$ excited state, which can give rise to luminescence.

Our group developed a cerium photocatalyst $(Cp^{Me4})_2Ce(\mathbf{L})$ (**1-Ce**, $Cp^{Me4} = C_5Me_4H$, **L**= [2-O-3,5-^{t}Bu$_2$-C$_6$H$_2$(1-C{N(CH)$_2$N(^{i}Pr)})]) that combines the photoexcitable Ce(III) with tunable ligands, to functionalize inert sp³ C–F bonds (Figure 1, top).[16] Notably, the redox non-innocent ligand **L** allowed us to extend this reactivity to typically photo- and redox-inactive lanthanum and the oxidation of **L** or a Cp^{Me4} ligand allows for turnover. Importantly, in order to cleave the strong C–F bond, **L** is required, and little reactivity is observed when using $(Cp^{Me4})_3Ce$ (**2-Ce**).[16]

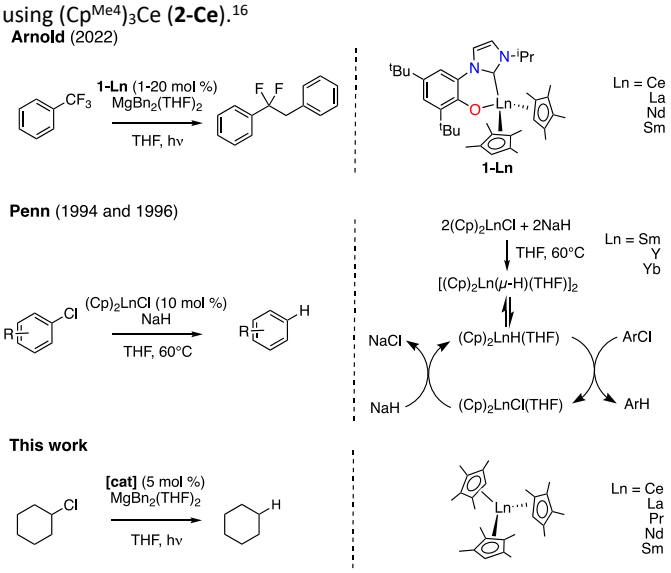

Figure 1 – Our photocatalytic C–F bond functionalization by complexes **1-Ln** (Ln = Ce, La, Pr, Nd, Sm) (top), dechlorination of aromatic chlorides by Cp_2LnCl complexes ($Cp = C_5H_5$, Ln = Y, Yb, Sm) carried out by Penn et al. (middle), and this work (bottom).

We were interested in Penn and co-workers' report that Cp_2LnCl complexes ($Cp = C_5H_5$ Ln = Y, Yb, Sm) could catalyze the dechlorination of activated aromatic chlorides with NaH (suspension in THF) at 60°C; they proposed a lanthanide hydride species as the active catalyst (Figure 1, middle).[17,18] This, and the ability of our complexes to cleave C–F bonds encouraged us to target functionalization of the unactivated alkyl C–Cl bond that has so far been outside the reach of other lanthanide-based visible light photocatalysts. This could be of utility in the chemical upcycling of polyvinyl chloride (PVC).[19,20] Globally, approximately 40 million tons of PVC are produced a year, yet a low percentage is recycled and the majority is through mechanical recycling in spite of its high energy demands.[21,22] Incineration or thermal degradation of PVC can release toxic by-products; low-energy dechlorination routes that would facilitate its conversion to useful products are desirable.[23]

Since previous work has implicated both cyclopentadienyl and chlorine radicals in photocatalytic bond activation,[14,16,24,25] and recognizing that the Cp ligand has some capacity for light absorbance,[26] we hypothesized that sp² and sp³ C–Cl bond activation could even be possible for other lanthanide Cp complexes, especially since the bond dissociation energy for the C–Cl bond is approximately 140 kJmol^{-1} weaker than the C–F bond.[27] Here, we show that lanthanide cyclopentadienyl complexes are efficient photocatalysts for the dechlorination of unactivated sp² C–Cl and sp³ C–Cl bonds in chlorohydrocarbons (Figure 1, bottom).

We chose to test the simple, robust, and soluble $(Cp^{Me4})_3Ln$ (**2-Ln** (Ln = La, Ce, Pr, Nd, Sm, Dy) and $[(Cp^{Me4})_2Ln(\mu\text{–}Cl)]_2$ **3-Ln** (Ln = Ce,[16] Nd, Sm) to probe this catalysis.[17,18] Complex **1-Ce** was also tested for comparison as it is so effective at C–F bond cleavage. All new complexes have been fully characterized (see ESI). The dialkyl $MgBn_2(THF)_2$ is used to turn over the catalysis, as it is THF-soluble (c.f. insoluble NaH), and was efficient as a reductant and coupling partner in photocatalytic C–F bond activation and functionalization.[16] The catalysis procedure consists of dissolution of the chosen Ln complex in THF with 20 equivalents of chlorohydrocarbon and $MgBn_2(THF)_2$, exposure to 440 nm light from a low energy Kessil lamp, and the reaction is monitored by NMR spectroscopy.

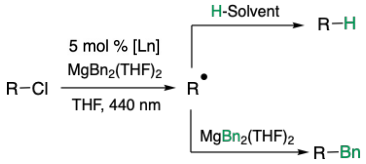

Scheme 1 - General reactions for C–Cl activation and hydrodechlorination by **1-Ln, 2-Ln** and **3-Ln**. Following C–Cl bond cleavage the C radical can be quenched by abstraction of H radical from solvent, or a benzyl radical from turnover reagent $MgBn_2(THF)_2$.

The anticipated reactions are shown in Scheme 1. Light absorption occurs first, presumably by the Cp^{Me4} ligand or the cerium cation if present, see later calculations. If this generates an excited state complex that is sufficiently reducing to cleave the R–Cl bond, then the reaction should release the R radical, to be trapped by solvent (R–H, scheme 1 upper) or a Bn group from the $MgBn_2(THF)_2$ co-reagent (R–Bn, scheme 1 lower). We explored the substrate scope of dechlorination to include allyl, vinyl, primary, secondary and tertiary carbon centers, substituted chloroarenes, and commercial PVC (polyvinyl chloride) polymer, as discussed in the ESI and below.

For the substrates chlorocyclohexane (a simple model for PVC) and 1-chloro-2-methylpropene, the radical formed from Cl atom abstraction is short-lived, and the organic product is the hydrocarbon arising from replacement of Cl by H. This is confirmed by ^{1}H NMR spectroscopy. The H atom derives from the THF solvent, Scheme 1, upper.[16] This was corroborated by carrying out reactions with 1-chloro-2-methylpropene and chlorocyclohexane in THF-D_8; deuterium- incorporated 2-methylpropene and cyclohexane respectively were identified by ^{13}C NMR spectroscopy. As with our previously reported photocatalytic defluorination chemistry, there is a significant kinetic isotope effect in these reactions.[16]

In contrast, the reactions with substrates that produce a more stabilized radical intermediate following dechlorination yield a benzylated product, from reaction with the $MgBn_2(THF)_2$ or benzyl radicals in solution. The major product generated from dechlorination of 3-chloro-2-methylpropene by **2-Ce** is 3-methyl(but-3-en-1-yl)benzene, arising from the benzylation of the allyl radical.

The yields of cyclohexane produced by the lanthanide catalysts are shown in Figure 2. Additional data using a range of catalysts at different loadings, and additional substrates, are in the ESI alongside photophysical characterization of **3-Ce**. No substrate reaction is observed without UV light, or if the catalyst is replaced with $Mg(Cp^{Me4})_2$.

Of the Ce catalysts, **2-Ce** is best at dechlorination, generating cyclohexane in 93% yield after 24 hours irradiation. In catalyses involving **2-Ln** the chloride-containing complex **3-Ln** is recovered at the end. The chloride complex **3-Ce** is also a very good catalyst for this transformation, producing cyclohexane in 76% yield within the same time frame. Conversely, phenoxy-NHC complex **1-Ce**, a far superior catalyst to **2-Ce** for C–F bond activation,[16] produces cyclohexane in just 37% yield. **2-La** is also capable of the C–Cl bond activation, albeit less effectively, with 29% conversion.

All the cerium complexes are better catalysts than the other Ln congeners, in line with the straightforward, allowed excitation of the f^1 to a strongly reducing d^1 centered excited state. Because the Cp^{Me4} ligands can absorb light, all the early lanthanides can be photoexcited and their photocatalytic activity decreases with increasing atomic number. The heaviest lanthanide studied, **2-Dy,** produces negligible dechlorinated product, consistent with the requirement for the chlorinated substrate to bind the Ln, which is increasingly hindered in catalysts with smaller ionic radii.[28] Though rare, molecular complexes of tetravalent praseodymium are known.[29] Thus, it is possible that a Pr congener could be an efficient catalyst by effectively stabilizing a Ln(IV) intermediate. Catalyst **2-Pr** produces cyclohexane in 20% yield, which is in line with the increased stability of Ce(IV) relative to Pr(IV) and supports the value of the facile 4*f* → 5*d* excitation in the best catalysts.

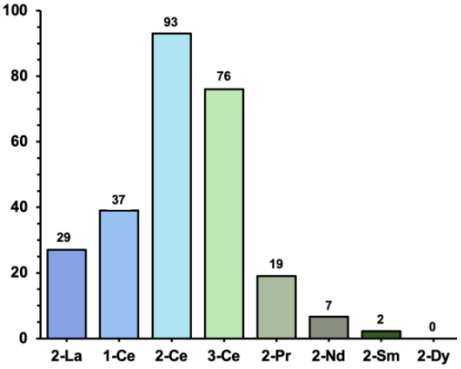

Figure 2 - Hydrodechlorination of chlorocyclohexane catalyzed by different Ln photocatalysts. Reactions were carried out at RT, in THF-H_8, with 5 mol % catalyst loading, and irradiated with a 40 W Kessil 440 nm lamp. The percentage yield of cyclohexane was determined by ^{1}H NMR spectroscopy relative to an internal standard.

A series of stoichiometric reactions give more insight into the mechanism of dechlorination by **2-Ce**. Even without irradiation, green THF solutions of **2-Ce** react with $MgBn_2(THF)_2$ turning the solution yellow-green due to the formation of the cerium benzyl species $(Cp^{Me4})_2Ce(Bn)(THF)$ (**4-Ce**), confirmed by ^{1}H NMR spectroscopy and an independent synthesis.[16] Spectroscopic measurements confirm that the four compounds **2-Ce**, **4-Ce**, $MgBn_2(THF)_2$ and $Mg(Cp^{Me4})_2$ are all present in equilibrium in solution at the start of the reaction.[30] A reaction of **2-Ce** with a 20-fold excess of $MgBn_2(THF)_2$ results in a mixture of these products with a calculated equilibrium constant of 2.5 for the equation in Figure 3, top. Product yields for both **2-Ce** and **3-Ce** are higher at lower catalyst loadings, which we attribute to the greater effective concentration of $MgBn_2(THF)_2$ that pushes the equilibrium towards the active species **4-Ce** (see ESI). This is not seen for **1-Ce**, as the chelating aryloxy-NHC ligand complex is less susceptible to ligand exchange with benzyl radicals, as we showed in our previous study. For the series **2-Ln** other than Ce, the anticipated increase in product formation with increasing catalyst loading is as would be anticipated.

The addition of chlorohydrocarbon substrate to the mixture containing **2-Ce** and **4-Ce** and irradiation for 24 hours generates a bright yellow solution arising from the complete conversion to the chloride complex **3-Ce** which is identified by ^{1}H NMR spectroscopy (Figure 3, top right). We experimentally verified that irradiation of a pure sample of **4-Ce** results in the formation of **2-Ce** and bibenzyl (Figure 3, middle) and the reaction of **3-Ce** and $MgBn_2(THF)_2$ to form

the benzyl **4-Ce** does not proceed without irradiation, *vide infra* (Figure 3, bottom).

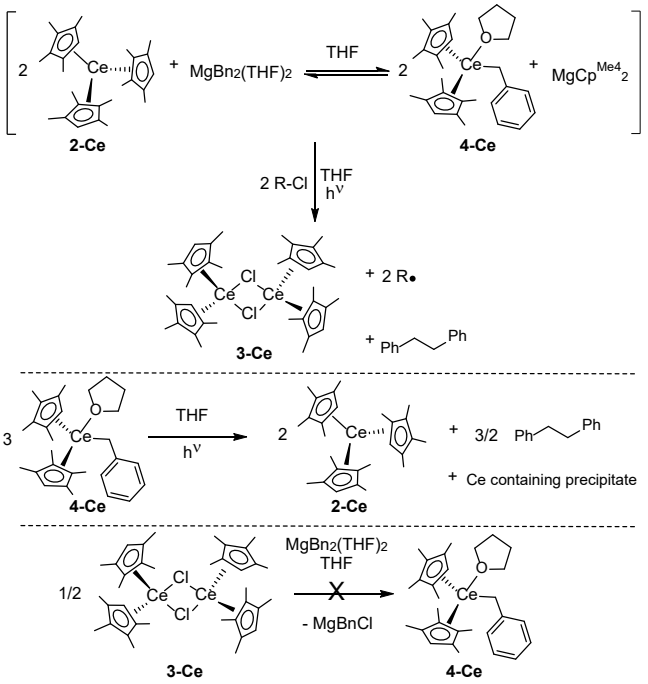

Figure 3 – Stoichiometric reactions to define the mechanism of C–Cl activation by **2-Ce**.

Schelter and co-workers showed that Ce(III) amido and guanidinate photocatalysts form an inner-sphere complex with benzyl chloride, which lowers the barrier to halogen atom abstraction, and releases benzyl radical to form products.[28] Here, calculations were performed for the excited states of complexes **2-Ce** and **2-La** and the proposed intermediate in which cyclohexylchloride binds as a Cl–donor ligand to **4-Ce**, recognizing that both the tris(Cp) and benzyl complex can be active catalysts.

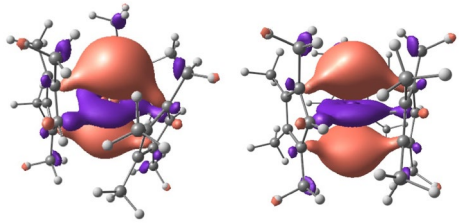

Figure 4 - Depictions of the calculated SOMO of **2-Ce** (left) and **2-La** (right) after absorption. Color code: gold – Ce; green – Cl; grey – C; white – H.

Time-dependent DFT (TD-DFT; B3PW91) calculations on both **2-Ce** and **2-La** reveal similar SOMO structures upon photoexcitation (Figure 4). Experimentally, both **2-Ce** and **2-La** absorb at 426 nm, calculated as an intense absorption at approximately 380 nm (415nm in solvent).[31] This is assigned as transition from the π orbital of the Cp^{Me4} ligand to the dz^2 on the metal. For **2-Ce**, this is accompanied by a lower intensity metal-based $4f \rightarrow 5d$ excitation at 410 nm. It is notable that the calculated geometry of the photoexcited **2-Ce** is pyramidally distorted by 5° away from the ground state pseudo-D_{3h} symmetry, unlike the La congener. This increases access to one end of what was a primarily dz^2-orbital, and we suggest this may provide greater access to the Cl substrate, or the Bn reagent, which would further contribute to the higher activity of Ce relative to La, despite its smaller ionic radius.

TD-DFT studies of the Cl–alkyl adduct of **4-Ce** show a low intensity absorption at 425 nm (448 nm calculated with an added solvent correction), experimentally observed at 450 nm, arising from the excitation of the SOMO ($4f$ electron) into the LUMO which is primarily bonding for the Ce–Cl bond and antibonding with respect to the C–Cl bond (Figure 5). supports our experimental observation that **4-Ce** cannot be formed from **3-Ce** without irradiation, and could be attributed to the strength of the Ce–Cl bond relative to Ce–C. The excited state populated by irradiation also implies the transition from the HOMO, which is the Ce–Bn bonding interaction, to the LUMO so that the Ce–Bn bond may easily be broken. This early loss of the Bn group is consistent with our observations of the difficulty of trapping it in a product when substrates with short-lived radical products are used.

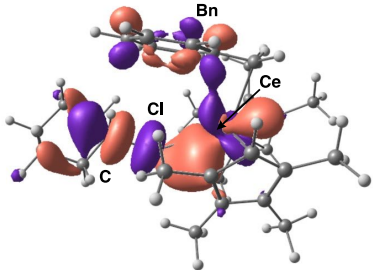

Figure 5 - The TD-DFT-calculated LUMO of the adduct formed during catalysis when chlorocyclohexane binds to **4-Ce** . Color code: gold – Ce; green – Cl; grey – C; white – H.

Our proposed mechanism therefore begins with the formation of a mixture of **2-Ce** and **4-Ce** and excess $MgBn_2(THF)_2$. The added chloroalkane will bind as an L–donor, most likely to the less sterically saturated Ln center in **4-Ln**. Photoexcitation results in formation of the Ln–Cl bond as C–Cl bond cleavage occurs, releasing the hydrocarbyl radical R•. The intermediate $(Cp^{Me4}_2)Ln(Cl)(Bn)$ will be more stable for Ln = Ce, and to a much lesser extent Ln = Pr, which can form tetravalent complexes, but we previously showed how the Cp ligand can be oxidized in place of the Ln center, to stabilize the other Ln intermediates for which Ln(IV) is not accessible. The release of the reducing Bn• will still be facile. We had anticipated that the proximity of R• and Ln–Bn in the solvent cage would lead to the alkylated product R–Bn, but in THF, a good H-atom donor, R–H is formed through H atom abstraction from solvent when the resulting alkyl radical is unstabilized and too short-lived to be captured. Longer-lived allyl and benzyl radicals can be benzylated in this system, although we think that that this does not occur within the local coordination sphere of the lanthanide cation. The resulting chloride **3-Ln** is then photochemically converted back to the benzyl **4-Ln** by the excess $MgBn_2(THF)_2$ present.

This catalytic cycle is consistent with our experimental observations that the activities of precatalysts $(Cp^{Me4}_2)CeX$ (X = Cp^{Me4}, Cl, **L**) are related to the rate at which they can form alkyl species **4-Ce**. Catalyst **2-Ce** is more effective than **1-Ce** and **3-Ce** potentially due to the higher stability of the Ln–(O–NHC) and Ln–Cl bonds respectively relative to Ln–Cp^{Me4}.[16,32,33] It should also be noted that the excited state lifetime of **3-Ce** is 175 ns, which is amongst the longest excited state lifetimes reported for a cerium complex.[1] In contrast, the lifetime of **1-Ce** is considerably shorter at 101 ns, though still greater than many other Ce complexes studied.[34] Ultimately, while specialized, light-absorbing ligand **L** is required for cleaving the strong $C(sp^3)$–F bond, absorption through Cp^{Me4} is satisfactory for activation of the weaker $C(sp^3)$–Cl bond, providing evidence of the power of ligand-tuning of lanthanide photocatalysis.

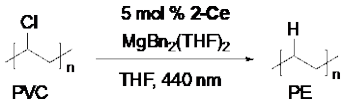

(1)

With an interest in polymer upcycling, preliminary results suggest that under standard conditions, **2-Ce** at 5 mol % loading can photocatalytically cleave 79% of the C–Cl bonds in a sample of PVC in a 24-hour period, eq. 1. As the dechlorination proceeds, the polymer becomes insoluble in THF and can thus be readily isolated (see figure S3). Extended reaction times and lower catalyst loadings

result in comparable yields, suggesting dechlorination progresses until the the polymer becomes insoluble in THF. FT-IR spectroscopy (see ESI) of the sample shows spectral features that correlate with segments of polyethylene, no evidence of polyacetylenic groups, and some level of unsaturation, which is also observed as a natural defect in commercial PVC. The insolubility of the polymer in organic solvents at high temperatures support the absence of chain shortening but have precluded characterization by GPC. Work to functionalize these materials at the site of radical formation are currently underway.

Author Contributions

A. E. K.: experiments, analysis, writing & editing. E.T.O.: solving X-ray data for **3-Nd**, **3-Sm**, A.P and S.N.K.: collection of X-ray data for **3-Nd**, **3-Sm**. P. L. A.: project conceptualization, funding acquisition, supervision, analysis, writing & editing. S.C: calculations, writing. L.M. supervision, writing.

Acknowledgments

The synthetic and catalytic parts of this research were supported by the Rare Earth Project in the Separations Program and the Catalysis Program respectively of U.S. Department of Energy (DOE), Office of Science, Office of Basic Energy Sciences, Chemical Sciences, Geosciences, and Biosciences Division. Dr C. Citek and the Catalysis Laboratory provided instrumentation. Drs R. J. Abergel, L. Arnedo Sanchez and J. Wacker helped with photophysical measurements. Drs B. Helms and J. Demarteau at the Molecular Foundry, a DOE Office of Science User Facility helped with polymer characterization. Xray data were collected at BL12.2.1 of the ALS, a DOE Office of Science User Facility. All the above are funded under DE-AC02-05CH11231. The CoC-NMR spectroscopy facility is supported in part by NIH S10OD024998; thanks to Dr H. Celik for help with NMR spectroscopy. L.M. is a senior member of the Institut Universitaire de France. The Chinese Academy of Science and the Chinese Scholarship Council are acknowledged for financial support for SC and LM; CALMIP is thanked for generous computing time.

Conflicts of interest

There are no conflicts of interest to declare.

Notes and references

‡ Electronic supplementary information (ESI) available: Additional experimental, computational data. Crystallographic datasets are available from the CCDC deposition numbers 2239626-2239627.

References

1 G. E. M. Crisenza and P. Melchiorre, *Nat. Commun*, 2020, **11**, 803.
2 J. W. Tucker and C. R. J. Stephenson, *J. Org. Chem.*, 2012, **77**, 1617–1622.
3 J. Twilton, C. C. Le, P. Zhang, M. H. Shaw, R. W. Evans and D. W. C. MacMillan, *Nat. Rev. Chem.*
4 K. P. S. Cheung, S. Sarkar and V. Gevorgyan, *Chem. Rev.*, 2022, **122**, 1543–1625.
5 J.-J. Guo, A. Hu, Y. Chen, J. Sun, H. Tang and Z. Zuo, *Angew. Chem. Int. Ed.*, 2016, **128**, 15545–15548.
6 T. Cheisson and E. J. Schelter, *Science*, 2019, **363**, 489–493.
7 P. L. Arnold, R. W. F. Kerr, C. Weetman, S. R. Docherty, J. Rieb, F. L. Cruickshank, K. Wang, C. Jandl, M. W. McMullon, A. Pöthig, F. E. Kühn and A. D. Smith, *Chem. Sci.*, 2018, **9**, 8035–8045.
8 R. W. F. Kerr, P. M. D. A. Ewing, S. K. Raman, A. D. Smith, C. K. Williams and P. L. Arnold, *ACS Catal.*, 2021, **11**, 1563–1569.
9 A. Ogawa, Y. Sumino, T. Nanke, S. Ohya, N. Sonoda and T. Hirao, *J. Am. Chem. Soc.*, 1997, **119**, 2745–2746.
10 T. C. Jenks, M. D. Bailey, J. L. Hovey, S. Fernando, G. Basnayake, M. E. Cross, W. Li and M. J. Allen, *Chem. Sci.*, 2018, **9**, 1273–1278.
11 T. Kondo, M. Akazome and Y. Watanabe, *J. Chem. Soc. Chem. Commun.*, 1991, 757–758.
12 A. Ogawa, S. Ohya, Y. Sumino, N. Sonoda and T. Hirao, *Tetrahedron Lett.*, 1997, **38**, 9017–9018.
13 Y. Qiao and E. J. Schelter, *Acc. Chem. Res.*, 2018, **51**, 2926–2936.
14 A. Hu, J. J. Guo, H. Pan and Z. Zuo, *Science*, 2018, **361**, 668–672.
15 A. Prieto and F. Jaroschik, *Curr. Org. Chem.*, 2021, **26**, 6–41.
16 A. E. Kynman, L. Elghanayan, A. Desnoyer, Y. Yang, L. Severy, A. Di Giuseppe, T. D. Tilley, L. Maron and P. L. Arnold, *Chem. Sci.*, 2022, **13**, 14090–14100.
17 Deng, Dao, Li; Qian, Chang Tao; Penn, John H., *Chin. Chem. Lett.*, 1994, **5**, 303–304.
18 Penn, John H.; Li Deng, Dao; Qian, Chang Tao, *Chin. Chem. Lett.*, 1996, **7**, 845–846.
19 Q. Hou, M. Zhen, H. Qian, Y. Nie, X. Bai, T. Xia, M. Laiq Ur Rehman, Q. Li and M. Ju, *Cell Rep. Phys. Sci.*, 2021, **2**, 100514.
20 X. Zhao, B. Boruah, K. F. Chin, M. Đokić, J. M. Modak and H. S. Soo, *Adv. Mater.*
21 R. Geyer, J. R. Jambeck and K. L. Law, *Sci. Adv.*, 2017, **3**, e1700782.
22 M. F. Ashby, *Materials and sustainable development*, Butterworth-Heinemann, Oxford, Second edition., 2023.
23 A. M. Hapipi, H. Suda, Md. A. Uddin and Y. Kato, *Energy Fuels*, 2018, **32**, 7792–7799.
24 Q. Yang, Y.-H. Wang, Y. Qiao, M. Gau, P. J. Carroll, P. J. Walsh and E. J. Schelter, *Science*, 2021, **372**, 847–852.
25 Q. An, Y.-Y. Xing, R. Pu, M. Jia, Y. Chen, A. Hu, S.-Q. Zhang, N. Yu, J. Du, Y. Zhang, J. Chen, W. Liu, X. Hong and Z. Zuo, *J. Am. Chem. Soc.*, 2023, **145**, 359–376.
26 M. E. Fieser, J. E. Bates, J. W. Ziller, F. Furche and W. J. Evans, *J. Am. Chem. Soc.*, 2013, **135**, 3804–3807.
27 *CRC Handbook of Chemistry and Physics*, CRC Press, 2022.
28 H. Yin, P. J. Carroll, B. C. Manor, J. M. Anna and E. J. Schelter, *J. Am. Chem. Soc.*, 2016, **138**, 5984–5993.
29 A. R. Willauer, C. T. Palumbo, F. Fadaei-Tirani, I. Zivkovic, I. Douair, L. Maron and M. Mazzanti, *J. Am. Chem. Soc.*, 2020, **142**, 5538–5542.
30 Y. Yao and Q. Shen, in *Rare Earth Coordination Chemistry*, ed. C. Huang, John Wiley & Sons, Ltd, Chichester, UK, 2010, pp. 309–353.
31 H.-D. Amberger and H. Reddmann, *Z. anorg. allg. Chem.*, 2008, **634**, 173–180.
32 P. L. Watson, T. H. Tulip and I. Williams, *Organometallics*, 1990, **9**, 1999–2009.
33 M. E. Fieser, C. W. Johnson, J. E. Bates, J. W. Ziller, F. Furche and W. J. Evans, *Organometallics*, 2015, **34**, 4387–4393.
34 P. Pandey, Q. Yang, M. R. Gau and E. J. Schelter, *Dalton Trans.*, 2023, **52**, 5909–5917.